Draft version October 1, 2018
Typeset using LaTeX **manuscript** style in AASTeX62

Three-Dimensional Oscillations of Twenty One Halo Coronal Mass Ejections by Multi-Spacecraft

Harim Lee,[1] Y.-J. Moon,[1,2] V. M. Nakariakov,[1,3] Hyeonock Na,[1] Il-Hyun Cho,[2] and Eunsu Park[1]

[1]*School of Space Research, Kyung Hee University, Yongin 17104, Korea*

[2]*Department of Astronomy and Space Science, Kyung Hee University, Yongin 17104, Korea*

[3]*Centre for Fusion, Space & Astrophysics, Physics Department, University of Warwick, Coventry CV4 7AL, UK*

(Received; Revised ..; Accepted October 1, 2018)

Submitted to ApJ

ABSTRACT

We investigate the 3D structure of kinematic oscillations of full halo coronal mass ejections (FHCMEs) using multi-spacecraft coronagraph data from two non-parallel lines-of-sight. For this, we consider 21 FHCMEs which are simultaneously observed by SOHO and STEREO A or B, from August 2010 to August 2012 when the spacecraft were roughly in quadrature. Using sequences of running difference images, we estimate the instantaneous projected speeds of the FHCMEs at 24 different azimuthal angles in the planes of the sky of those coronagraphs. We find that all these FHCMEs have experienced kinematic oscillations characterized by quasi-periodic variations of the instantaneous projected radial velocity with the periods ranging from 24 to 48 minutes. The oscillations detected in the analyzed events are found to show distinct azimuthal wave modes. Thirteen events (about 62%) are found to oscillate with the azimuthal

Corresponding author: Yong-Jae Moon
moonyj@khu.ac.kr

wave number $m = 1$. The oscillating directions of the nodes of the $m = 1$ mode for these FHCMEs are quite consistent with those of their position angles (or the direction of eruption), with the mean difference of about 23 degrees. The oscillation amplitude is found to correlate well with the projected radial speed of the coronal mass ejection. An estimation of Lorentz accelerations shows that they are dominant over other forces, implying that the magnetic force be responsible for the kinematic oscillations of coronal mass ejections. However, we may not rule out other possibilities: a global layer of enhanced current around the CMEs or non-linear nature of its driver, for example, the effect of vortex shedding.

Keywords: Sun: coronal mass ejections (CMEs) — Sun: oscillations

1. INTRODUCTION

Coronal mass ejections (CMEs) are the most spectacular eruptions from the Sun into the heliosphere. They are usually thought to be the main source of strong geomagnetic storms (e.g., Gosling et al. 1991; Gosling 1993). It has been well known that the interplanetary propagation of CMEs is controlled by the ambient solar wind (e.g., Lindsay et al. 1999; Gopalswamy et al. 2000, 2001a,b; Vršnak & Žic 2007). Several authors (e.g., Vršnak et al. 2004; Yashiro et al. 2004) suggested that the interaction between CMEs and the solar wind is an important mechanism that determines CME kinematics.

Dynamical processes in the solar corona are often accompanied by the excitation of various kinds of oscillations of coronal plasma non-uniformities, with the periods ranging from a fraction of a second to several hours. The majority of coronal oscillations have been identified as magnetohydrodynamic (MHD) modes of various plasma non-uniformities (see, e.g., De Moortel & Nakariakov 2012; Liu & Ofman 2014, for comprehensive reviews). The interest in MHD oscillations is related to many open questions, such as heating of the plasma, the presence of additional sinks for the energy released in flares, triggering the energy releases, and MHD seismology — diagnostics of plasma parameters and physical processes operating in the plasma by means of MHD oscillations.

CMEs may be accompanied by MHD oscillations that appear naturally as the response of the elastic and compressive plasma to the energy deposition. The first observation of oscillations in CME kinematics was reported by Krall et al. (2001). Examining the evolution of the speed patterns of the leading-edge and trailing-edge features for a flux-rope-like CME, they found that the projected CME speeds varied with the period of about 4–6 hr. Shanmugaraju et al. (2010) examined the speed–distance profiles of 116 CMEs observed with at least 10 height–time data points, and found that the about fifteen CMEs had quasi-periodic oscillation patterns in the evolution of their speed. The oscillation periods were estimated to be within the range of the upper and lower limit of the Alfvén travel times along the magnetic ropes of CMEs. Lee et al. (2015) presented the first detection of both radial and azimuthal oscillations in halo CMEs (HCMEs) observed by LASCO C3. They found that the instantaneous projected radial velocity varies quasi-periodically, with the period ranging from 24 to 48 minutes, and that the oscillations of seven CMEs are associated with distinct $m = 1$ azimuthal wave modes, where m is the azimuthal wave number. Michalek et al. (2016) performed a comprehensive statistical study on the kinematics of 187 limb CMEs observed with LASCO. They found that 22% of the CMEs observed in 1996–2004 years revealed periodic variations of the projected radial acceleration and speed, with the average amplitude 87 km s^{-1}, mean period 241 minutes and wavelength 7.8 $R_\odot$.

Lee et al. (2015) suggested that the kinematic oscillations of CMEs could be associated with a "zigzag" trajectory of the plasmoid, caused by the periodic shedding of vortices from its alternate sides in the direction perpendicular to the path (Nakariakov et al. 2009). In this scenario, the oscillation period anti-correlates with the CME speed, which was found to be consistent with observations. Michalek et al. (2016) concluded that properties of CME oscillations are consistent with the thin magnetic rope oscillation model of Cargill et al. (1994). Recently, Takahashi et al. (2017) developed a theoretical model of quasi-periodic oscillations of CME ropes, based on time-dependent magnetic reconnection in eruptive flares. The oscillation period was estimated as the ratio of the width of the reconnection outflow near the CME flux rope, and the Alfvén speed in the inflow region near the stagnation point, multiplied by an empirically determined factor of about 20. This modeling

demonstrated the possibility of an oscillatory behavior of the CME radial and expansion speeds with the periods ranging from ten to several hundred minutes at a heliocentric distance of about 10 $R_\odot$. An important feature of this mechanism is the linear increase in the period with the distance from the Sun, which could be tested observationally.

Thus, many authors have shown a variety of oscillatory patterns in the CME kinematics using single spacecraft observations, revealing that it is a common feature of CME propagation. Those findings are supported by the results of theoretical estimations and modeling. However, single-view observations do not provide information about the 3D structure of the oscillations, as coronagraphic observations of CMEs are subject to projection effects (see, e.g. Bronarska & Michalek 2018, for a recent discussion). In particular, it is not clear whether the apparent oscillatory variations of the projected speed of CMEs are radial or azimuthal, i.e. whether the oscillations are polarised along or across the CME propagation direction. There has been so far no attempt to make a simultaneous observation of 3D CME oscillations using imaging observations from different lines-of-sight (LoS). In this paper, we present the first detection of both radial and azimuthal oscillations of full HCMEs using multi-spacecraft observations with non-parallel LoS, and determination of their wave modes. The paper is organized as follows. In Section 2, we describe the data and analysis. Results are given in Section 3. A brief summary and discussion are presented in Section 4.

2. DATA

In this study, we consider full HCMEs (FHCMEs) observed by the Solar and Heliospheric Observatory (SoHO) / the Large Angle SpectrosCopic Observatory (LASCO, Brueckner et al. 1995) C3 and the Solar TErrestrial Relations Observatory (STEREO, Kaiser et al. 2008))/ the Sun–Earth Connection Coronal and Heliospheric Investigation (SECCHI) COR2 from June 2011 to August 2012, when these space missions were approximately in quadrature. During this period of time, the angular separation of the STEREO-A and -B spacecraft from the Sun–Earth line was in the ranges of 94°–123° and 93°–115°, respectively. The field of view of LASCO C3 is 3.7–30 $R_\odot$, and that of STEREO COR2 is 2–15 $R_\odot$.

We choose 21 well-observed FHCMEs whose front structures are clearly seen in both C3 and COR2, and whose evolution was traced by at least five consecutive measurements, made at the heights from 3.2 to 26.8 $R_\odot$ with the time cadence of about 12–15 minutes. The dates, times, source locations and other properties of the events are summarized in Table 1.

Figure 1 shows running difference images of the 2011 September 22 event, obtained with three satellites: STEREO-B COR2, LASCO C3, and STEREO-A COR2. For each running difference image, we estimate locations of the FHCME's front edge at every 15° of the azimuthal angle (see Figure 1). The projected instantaneous speed $V_{\rm ins}$ of the FHCME was determined using two successive height-time measurements at every azimuthal angle.

Some uncertainties in determining the speed $V_{\rm ins}$ may exist because the determination of the HCME front edge locations are made by visual inspection. To estimate the uncertainty of the instantaneous speed estimation, we made ten independent trials of the measurements of the front edge locations, i.e. the technique used by Lee et al. (2015). Then the error is estimated as the standard deviation of those independent measurement, typically about 170 km s^{-1}.

To make the running difference images, we use Level 0.5 data obtained by the LASCO/EIT Images Query Form (https://sharpp.nrl.navy.mil/cgi-bin/swdbi/lasco/images/form), and the SECCHI Flight images Query Form (https://secchi.nrl.navy.mil/cgi-bin/swdbi/secchi_flight/images/form).

3. RESULTS AND DISCUSSION

Figure 2 gives an example of the instantaneous speed measurements, showing the speed as a function of time along different azimuths for the 2011 June 4 event, together with the best-fitting harmonic function. The speed is seen to quasi-periodically oscillate with the distance from the Sun, rather than monotonically increase or decrease. The apparent oscillation was fitted by a harmonic function $V_{\rm ins} = \Delta V \sin(\omega(t-K))+b$, where ΔV is the amplitude, ω is the cyclic frequency, K is the phase, and b is the mean value, which are determined by the least-square method. Following this approach, we estimate the speed amplitudes ΔV at every azimuth angle, stepping by 15°, of all events. We restrict our attention to the datasets which have the absolute values of the cross-correlation coefficients with the best-fitting harmonic functions larger than 0.6. For example, for the event shown in Fig. 2, the

CME speed evolution along a number of azimuthal rays positively correlates with the harmonic function, with the maximum cross-correlation coefficient $CC_{\rm max} = 0.99$ and the mean cross-correlation coefficient $CC_{\rm mean} = 0.91$. The speed variation along other azimuthal rays in this CME shows strong anti-correlation with this function, $CC_{\rm max} = -0.99$ and $CC_{\rm mean} = -0.90$. Following this procedure, we estimate instantaneous radial speeds at every 15° azimuthal direction, for 21 FHCMEs. We find that all the FHCMEs have oscillatory patterns in the instantaneous projected speeds. In addition, we estimate the maximum observed projected speeds $V_{\rm pro}$ of the FHCMEs, which are obtained from a linear fit of height-time data at every azimuthal angle. Parameters of the detected oscillations, and the CME speeds are given in Table 1.

Figure 3 shows an example in which the oscillatory pattern of instantaneous projected speeds has a systematic azimuthal dependence. This dependence occurs to be different if observed from different LoS, with LASCO C3 and STEREO-A COR2 in the CME shown in the figure. To quantify the azimuthal dependence of the oscillatory patterns, we estimate it as a harmonic function $\exp(im\theta)$, where θ is the azimuthal angle, and m is an integer representing the azimuthal wave number. The azimuthal wave number m is estimated by the following procedure: (1) according to the phase of the oscillations (see the left panels of Fig. 3) we group the oscillations at all azimuthal angles into the "positive", "negative", and "non-oscillatory" groups; (2) we position nodal lines between the azimuthal rays corresponding to the "positive" and "negative" groups; (3) the azimuthal mode number m of the oscillation is obtained as the number of the nodal lines. The instantaneous projected speed pattern along a given azimuthal angle is considered to belong to either "positive" or "negative" groups if it has the cross-correlation coefficient with the best-fitting harmonic functions either larger than 0.6, or smaller than −0.6, respectively. The oscillation position angle (OPA) is defined as a position angle of the direction that is perpendicular to the nodal line for $m = 1$, and 45° from the nodal line for $m = 2$.

As seen in the left panel of Fig. 3a, the oscillatory patterns observed with LASCO C3 in all azimuthal angles have the same phase, and hence positively correlate with the same harmonic function. As seen in the left panel of Fig. 3b, the oscillatory patterns observed with STEREO-A COR2 have,

depending upon the azimuthal angle, two opposite phases. In the "positive" group of the azimuths the oscillations correlate positively with a chosen harmonic function, while oscillations that belong to the "negative" group correlate with this function negatively. As seen in the right panel of Fig. 3, the azimuthal distribution of the "positive" and "negative" groups observed with COR2 indicates the $m = 1$ mode. Thus, in this CME the oscillatory pattern observed with LASCO C3 corresponds to the $m = 0$ mode, while the oscillation observed from another LoS, with STEREO-A COR2, corresponds to the $m = 1$ mode. The oscillatory patterns are presented in more than 50% of the azimuthal angles. The observed maximum projected speed are found to be about 2,900 $\mathrm{km\,s^{-1}}$ for LASCO C3 and about 2,200 $\mathrm{km\,s^{-1}}$ for STEREO-A COR2, respectively. The instantaneous speed oscillation amplitude are estimated to be about 970 $\mathrm{km\,s^{-1}}$ for LASCO C3 and about 700 $\mathrm{km\,s^{-1}}$ for STEREO-A COR2, respectively. The oscillation period of the FHCME is about 24 minutes for LASCO C3 and 30 minutes for STEREO-A COR2.

Figure 4 gives an example of a CME with another azimuthal oscillatory pattern. As seen in the right panel of Fig. 4, the oscillatory patterns are clearly presented for more than 50% of the azimuthal angles. The observed maximum projected speeds are found to be about 2,700 $\mathrm{km\,s^{-1}}$ for LASCO C3, and about 2,300 $\mathrm{km\,s^{-1}}$ for STEREO-B COR2, respectively. The instantaneous speed oscillation amplitudes are found to be about 700 $\mathrm{km\,s^{-1}}$ for LASCO C3 and about 600 $\mathrm{km\,s^{-1}}$ for STEREO-B COR2, respectively. The oscillation period of the FHCME is about 24 minutes for LASCO C3, and 30 minutes for STEREO-B COR2. As seen in the left panel of Fig. 4, the oscillatory patterns have two opposite phases: positive correlations at some azimuthal angles and negative correlations at the other angles with the same harmonic function. Thus, the oscillation observed in this event is likely of the $m = 2$ mode from the LASCO C3 LoS, and the $m = 1$ mode from the COR2 LoS.

Figure 5 shows a sketch of the possible 3D structure of the kinematic oscillation of the FHCME shown in Fig. 3. If the propagation direction of a CME and its oscillation direction are same, i.e. the oscillation is polarised in the radial (vertical) direction, and the CME is seen from the LoS parallel to this direction, oscillatory patterns along each azimuth should have the same phase (i.e., $m = 0$, see the LASCO view in Fig. 5). The same oscillatory pattern could look differently if seen

from another direction. In particular, the apparent oscillatory patterns on either sides of the CME may have opposite phases, i.e. the positive phase at one side and negative phase at the other side ($m = 1$), if the LoS is perpendicular to the oscillation polarisation direction, see the STEREO view in Fig. 5. This fact shows that when the propagation direction is close to the oscillation direction, its wave mode is not properly identified in the coronagraph observation with the LoS parallel to the propagation direction. In particular, an $m = 1$ mode would be seen as an $m = 0$ mode. Therefore, in the identification of the oscillation mode we take a higher azimuthal mode out of two possible modes determined with different observational angles. Results obtained by this procedure for all 21 FHCMEs analyzed in this study are summarized in Table 1.

Figure 6a shows a relationship between the OPAs determined in this study and the measurement position angles (MPA, obtained from the LASCO catalogue) that corresponds to the projected directions of solar eruptions. In this plot, we use 13 events (ten events for $m = 1$ and three events for $m = 2$), and neglected 9 other events that either are of $m = 0$ or ambiguous. We find that the OPAs are quite consistent with the MPAs with the correlation coefficient of 0.92, and the mean absolute difference of 23°. This finding indicates that kinematic oscillations of these FHCMEs are mainly related to solar eruptions. Figure 6b shows a relationship between the oscillation amplitude and the maximum projected speed determined with LASCO C3. We find that there is a good correlation between these two quantities with the correlation coefficient of 0.80.

The net acceleration ($a_{\rm n}$) of a CME consists of the combination of the Lorentz acceleration ($a_{\rm L}$), gravitational acceleration ($g = 274/R^2$), and the aerodynamic drag acceleration ($a_{\rm d}$) (Cargill et al. 1996; Cargill 2004; Vršnak et al. 2004, 2010)

$$a_{\rm n} = a_{\rm L} - g + a_{\rm d} = a_{\rm L} - g - \gamma(v - w)|v - w|, \tag{1}$$

where γ is a drag parameter, v is the CME speed, and w is the ambient solar wind speed. The parameter γ (cm^{-1}) is given by

$$\gamma = C_d \frac{A\rho_w}{m}, \tag{2}$$

where C_d represents the dimensionless drag coefficient, A is the cross section area of the CME perpendicular to the direction of the propagation, ρ_w is the ambient solar wind density, and m is the CME mass. To estimate these parameters, we use the equations (3)-(6) of Vršnak et al. (2010). The mass of CME was estimated from brightness in LASCO C3 images (for details see Vourlidas et al. 2000, 2010). The Lorentz acceleration can be estimated by using $a_{\rm n}$ estimated from the CME speed profile, the drag parameter γ given by Vršnak et al. (2010), and $w = 400$ km s^{-1}. Figure 7 shows the instantaneous projected speed and the estimations of these three accelerations as a function of time for the analysed event. As seen in the figure, the Lorentz acceleration is dominant over the other ones so that it can be approximated as the net acceleration, which is the derivative of a CME speed. It is also noted that the effect of the drag force may be underestimated or overestimated due to the uncertainties of the drag coefficient and CME mass (Vourlidas et al. 2000, 2010; Sachdeva et al. 2015). Usually, the propagation phase of fast CMEs starts from a few solar radii (Vršnak 2006; Bein et al. 2011; Carley et al. 2012; Sachdeva et al. 2017). At large heights, the dynamics of CMEs has been assumed to be dominated by the aerodynamic drag (Gopalswamy et al. 2000, 2001a; Vršnak & Gopalswamy 2002; Yashiro et al. 2004; Tappin 2006; Manoharan 2006; Vršnak & Žic 2007; Vršnak et al. 2008, 2010; Subramanian et al. 2012; Sachdeva et al. 2015; Takahashi & Shibata 2017). Our results are inconsistent with the assumption of the past studies. We may conjecture a possibility that there is a global layer of enhanced current around the CMEs. Another possibility is that the kinematic oscillation is the result of local or non-linear nature of its driver as proposed in Nakariakov et al. (2009) and Takahashi et al. (2017).

4. SUMMARY AND CONCLUSION

Our study has shown the periodic variation of the instantaneous projected speed of FHCMEs, and allowed for determining the modes of the oscillation polarization, based on the imaging coronagraph observations from different LoS, obtained simultaneously with different spacecraft. We consider 21 FHCMEs, which were simultaneously observed by SOHO and STEREO A & B from August 2010 to August 2012 when the spacecraft were roughly in quadrature. We estimate the instantaneous speeds of the FHCMEs at 24 different azimuthal angles from the solar center in the plane of the sky. We

find that all these FHCMEs have experienced quasi-periodic variations of the instantaneous projected velocity. The oscillation amplitude is found to correlate well with the projected speed. Durations of the observed oscillations are found to range from 48 to 120 minutes. The oscillation period ranges from 24 to 48 minutes with the average of 33.3 minutes. The range of the detected periods is restricted by the time resolution of the coronagraphs used, and the duration of the detection. The oscillations of 21 events are found to be associated with distinct azimuthal wave modes, and the $m = 1$ mode is dominant (13 events, 62%).

Properties of the kinematic oscillation patterns determined in this study, i.e. the periods, amplitudes, and durations, are similar to those reported by Krall et al. (2001), Shanmugaraju et al. (2010), Lee et al. (2015), and Michalek et al. (2016). In particular, Lee et al. (2015) determined projected azimuthal wave modes of nine HCMEs. However, previous studies of this phenomenon were performed from a single LoS only, with the LASCO coronagraph, which did not allow the authors to account for the projection effects in the identification of the azimuthal mode of oscillation. The present study based on the use of observations of the oscillations from different LoS with different spacecraft, reduces the ambiguity of the azimuthal wave number identification. The oscillations are found to be polarized in the direction of the CME propagation. Oscillations of this polarization have already been detected at much smaller scale as vertical oscillations of a magnetic flux rope rising up in the corona (Kim et al. 2014). Estimations of the accelerations of the detected CMEs demonstrated that the effect of the Lorentz force is dominant over other forces such as the gravity and drag force. Thus, the magnetic force is likely to be responsible for the kinematic oscillations, and that the oscillations could be modeled by the approach introduced in (Cargill et al. 1994). On the other hand, the dependence of the oscillation amplitude on the CME speed, confirmed by this study, indicate a nonlinear nature of the oscillations (Nakariakov et al. 2009; Takahashi et al. 2017), associated with the vortex shedding phenomenon (Lee et al. 2015). However, the radial (vertical) polarization of the detected oscillations does not seem to be consistent with the intrinsically perpendicular (horizontal) direction of the vortex shedding phenomenon (Nakariakov et al. 2009). Our findings indicate the need for the

further development of the theory of kinematic oscillations of CMEs, in particular, accounting for their 3D nature and nonlinearity.

This work was supported by the BK21 plus program through the National Research Foundation (NRF) funded by the Ministry of Education of Korea, the Basic Science Research Program through the NRF funded by the Ministry of Education (NRF-2016R1A2B4013131), NRF of Korea Grant funded by the Korean Government (NRF-2013M1A3A3A02042232), the Korea Astronomy and Space Science Institute under the R&D program supervised by the Ministry of Science, ICT and Future Planning, the Korea Astronomy and Space Science Institute under the R&D program 'Development of a Solar Coronagraph on International Space Station (Project No. 2017-1-851-00)' supervised by the Ministry of Science, ICT and Future Planning, and Institute for Information & communications Technology Promotion(IITP) grant funded by the Korea government(MSIP) (2018-0-01422, Study on analysis and prediction technique of solar flares). V.M.N. acknowledges STFC consolidated grant ST/P000320/1.

The SOHO/LASCO CME catalog (http://cdaw.gsfc.nasa.gov/CME_list/) is generated and maintained at the CDAW Data Center by NASA and the Catholic University of America in cooperation with the Naval Research Laboratory. SOHO is a project of international cooperation between ESA and NASA. The STEREO/SECCHI data are produced by an international consortium of the NRL, LMSAL and NASA GSFC (USA), RAL and University of Birmingham (UK), MPS (Germany), CSL (Belgium), IOTA and IAS (France).

REFERENCES

Bein, B. M., Berkebile-Stoiser, S., Veronig, A. M., et al. 2011, ApJ, 738, 191

Bronarska, K., & Michalek, G. 2018, Advances in Space Research, 62, 408

Brueckner, G. E., Howard, R. A., Koomen, M. J., et al. 1995, SoPh, 162, 357

Cargill, P. J. 2004, SoPh, 338, 453

Cargill, P. J., Chen, J., & Garren, D. A. 1994, ApJ, 423, 854

Cargill, P. J., Chen, J., Spicer, D. S., & Zalesak, S. T. 1996, Geophys. Res., 101, 4855

Carley, Eoin P., McAteer, R. T. James, & Gallagher, Peter T. 2012, ApJ, 752, 36

De Moortel, I., & Nakariakov, V. M. 2012, Royal Society of London Philosophical Transactions Series A, 370, 3193

Gopalswamy, N., Lara, A., Lepping, R. P., et al. 2000, Geophys. Res. Let., 27. 145

Gopalswamy, N., Lara, A., Yashiro, S., Kaiser, M. L., & Howard, R. A., 2001a, J. Geophys. Res., 106, 29207

Gopalswamy, N., Yashiro, S., Kaiser, M. L., Howard, R. A., & Bougeret, J.-L. 2001b, J. Geophys. Res., 106, 29219

Gosling, J. T. 1993, J. Geophys. Res., 98, 18937

Gruszecki, M., Nakariakov, V. M., van Doorsselaere, T., & Arber, T. D. 2010, Physical Review Letters, 105, 055004

Gosling, J. T., McComas, D. J., Phillips, J. L., & Bame, S. J. 1991, J. Geophys. Res., 96, 7831

Kaiser, M. L., Kucera, T. A., Davila, J. M., St. Cyr, O. C., Guhathakurta, M., & Christian, E. 2008, Space Sci. Rev., 136, 5

Kim, S., Nakariakov, V. M., & Cho, K.-S. 2014, ApJL, 797, L22

Krall, J., Chen, J., Duffin, R. T., Howard, R. A., & Thompson, B. J. 2001, ApJ, 562, 1045

Lee, H., Moon, Y.-J., & Nakariakov, V. M. 2015, ApJL, 830, 1

Lindsay, G. M., Luhmann, J. G., Russell, C. T., & Gosling, J. T. 1999, SoPh, 104, 12515

Liu, W., & Ofman, L. 2014, SoPh, 289, 3233

Manoharan, P. K. 2006, SoPh, 235, 345

Michalek, G., Shanmugaraju, A., Gopalswamy, N., Yashiro, S., & Akiyama, S. 2016, SoPh, 291, 12

Nakariakov, V. M., Aschwanden, M. J., & Van Doorsselaere, T. 2009, A&A, 502, 661

Sachdeva, Nishtha, Subramanian, Prasad, Colaninno, Robin, & Vourlidas, Angelos 2015, ApJ, 809, 158

Sachdeva, Nishtha, Subramanian, Prasad, Vourlidas, Angelos, & Bothmer, Volker 2017, SoPh, 292, 118

Sheeley, N. R., Wang, Y.-M., Hawley, S. H., et al. 1997, ApJ, 484, 1

Shanmugaraju, A., Moon, Y.-J., Cho, K.-S., et al. 2010, ApJ, 708, 450S

Subramanian, Prasad, Lara, Alejandro, &Borgazzi, Andrea 2012, Geophys. Res. Lett., 39, 19107

Takahashi, T., & Shibata, K. 2017, ApJL, 837, L17

Takahashi, T., Qiu, J., & Shibata, K. 2017, ApJ, 848, 2

Tappin, S. J. 2006, SoPh, 233, 233

Vourlidas, A., Subramanian, P., Dere, K. P., & Howard, R. A. 2000, ApJ, 534, 456

Vourlidas, A., Howard, R. A., Esfandiari, E., Patsourakos, S., Yashiro, S. & Michalek, G. 2010, ApJ, 722, 1522

Vršnak, B. 2001, J. Geophys. Res.,106, A11

Vršnak, B. 2006, Adv. Space. Res., 38, 431

Vršnak, B., & Gopalswamy, N. 2002, J. Geophys. Res., Space Phys., 107, 1019

Vršnak, B., & Žic, T. 2007, Astron. and Astrophys., 472, 937

Vršnak, B., Ruždjak, D., Sudar, D., & Gopalswamy, N. 2004, Astron. and Astrophys., 423, 717

Vršnak, B., Vrbanec, D., & Čalogović, J. 2008, Astron. and Astrophys., 490, 811

Vršnak, B., Žic, T., Falkenberg, T. V., Möstl, C., Vennerstrom, S., & Vrbanec, D. 2004, Astron. and Astrophys., 512, 43

Yashiro, S., Gopalswamy, N., Michalek, G., et al. 2004, J. Geophys. Res., 109, 7105

Table 1. Oscillation parameters of 21 HCMEs

Date	Time (UT)	Location	MPA (deg)	OPA (deg)	Duration (minutes)		Distance ($R_\odot$)		Projected Speed V_{pro} (km s^{-1})		Speed Amplitude ΔV (km s^{-1})		Period (minutes)		Mode (m)			STEREO
					L	S	L	S	L	S	L	S	L	S	L	S	Final	
2011 Jun 4	06:48:06	N16W144	284	195, 285	60	60	5.8-25.2	4.7-16.1	2128	2002	768	425	24	30	2	0	2	A
2011 Aug 4	04:12:05	N19W36	298	300	120	60	5.1-24.7	3.8-15.1	2267	2185	717	539	24	30	1	1	1	A
2011 Sep 22	10:48:06	N09E89	72	90	72	60	5.5-21.7	4.3-11.9	2510	2241	776	492	24	30	1	1	1	B
2011 Sep 24	12:48:07	N10E56	78	-	72	75	4.9-27.0	3.9-15.7	2884	2163	967	695	24	30	0	1	1	A
2011 Oct 22	10:24:05	N25W77	311	-	96	90	9.6-24.9	4.1-13.6	1669	1332	565	346	48	30	0	1	1	B
2011 Nov 26	07:12:06	N17W49	327	-	120	60	6.4-25.5	3.6-15.8	1399	1639	506	563	48	30	-	0	-	A
2012 Jan 23	04:00:05	N28W21	326	330	60	60	5.4-21.8	3.2-13.8	2576	2568	590	939	24	30	1	2	2	A
2012 Jan 26	04:36:05	N41W84	327	-	60	60	4.9-25.7	3.3-11.6	2147	1744	756	482	24	30	0	1	1	A
2012 Jan 27	18:27:52	N27W71	296	195, 285	48	60	4.9-26.7	5.2-14.9	2657	2318	702	552	24	30	2	1	2	B
2012 Mar 5	04:00:05	N17E52	61	-	72	60	5.7-26.3	4.4-14.3	2451	1911	731	260	24	30	0	0	0	A
2012 Mar 10	18:00:05	N17W24	5	45	108	75	5.3-19.4	3.8-12.1	1825	1265	483	325	24	30	1	1	1	A
2012 Mar 13	17:36:05	N17W66	286	225	60	60	5.6-25.3	5.7-14.7	2398	1710	601	406	48	30	1	1	1	B
2012 Mar 18	00:24:05	N18W116	300	-	120	60	4.8-25.3	5.6-14.7	1496	1869	409	453	48	30	0	1	1	A
2012 Mar 26	23:12:05	N17E164	92	0, 90	48	60	4.2-15.4	6.8-16.4	1610	2022	430	422	24	30	2	1	2	B
2012 May 17	01:48:05	N11W76	261	-	60	60	5.7-25.8	5.6-14.5	2170	1619	745	531	24	30	-	1	-	B
2012 Jun 14	14:12:07	S17E06	144	120	120	60	5.3-17.6	3.8-14.7	1670	1777	567	360	24	30	1	1	1	A
2012 Jun 23	07:24:05	S11E60	290	-	84	60	5.0-27.4	6.5-14.7	2238	1045	628	211	24	30	-	1	-	B
2012 Jul 06	23:24:06	S13W59	233	255	48	60	5.0-26.8	5.3-16.0	2475	1949	828	454	48	30	1	0	1	B
2012 Jul 19	05:24:05	S13W88	275	210	72	60	4.6-24.3	3.3-14.7	2199	2544	744	580	24	30	1	0	1	A
2012 Jul 23	02:36:05	S17W132	286	270	72	60	4.4-24.7	4.6-15.7	2213	2598	644	458	24	30	1	0	1	A
2012 Aug 31	20:00:05	S25E59	90	135	72	75	4.2-18.8	4.4-15.1	1717	1557	509	297	24	30	1	0	1	A

NOTE—Columns 1–2: the CME first appearance date and time in the LASCO C2 field of view. Columns 3-4: the CME source location and measurement position angle (MPA) reported in the CDAW LASCO CME catalogue, respectively. Column 5: the CME oscillation position angle (OPA) in the LASCO C3 field of view. Columns 6-9: the CME observing duration and distance range for LASCO (L) and STEREO (S). Columns 10-13: the maximum projected CME speed (V_{pro}), and its oscillation amplitude (ΔV) for L and S. Columns 14-15: the CME oscillation periods for L and S. Columns 16-19: the azimuthal mode number of the CME oscillation for L, S, and combined. Column 20: STEREO-A or -B. If the field is blank (or has a dash), it means a rather complex wave pattern.

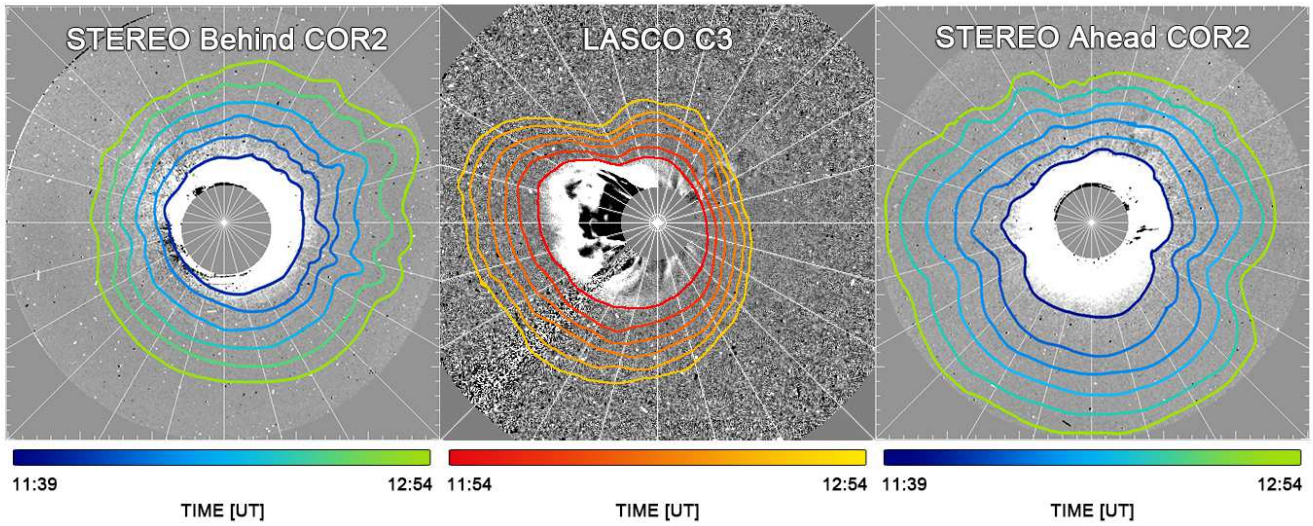

Figure 1. Running difference images of the 2011 September 22 FHCME at 11:39 - 12:54 UT. All measurements are made at every 15° (white lines). The color contour lines show the locations of the front edges of the FHCME from STEREO B COR2 (Left), LASCO C3 (Middle) and STEREO A COR2 (Right).

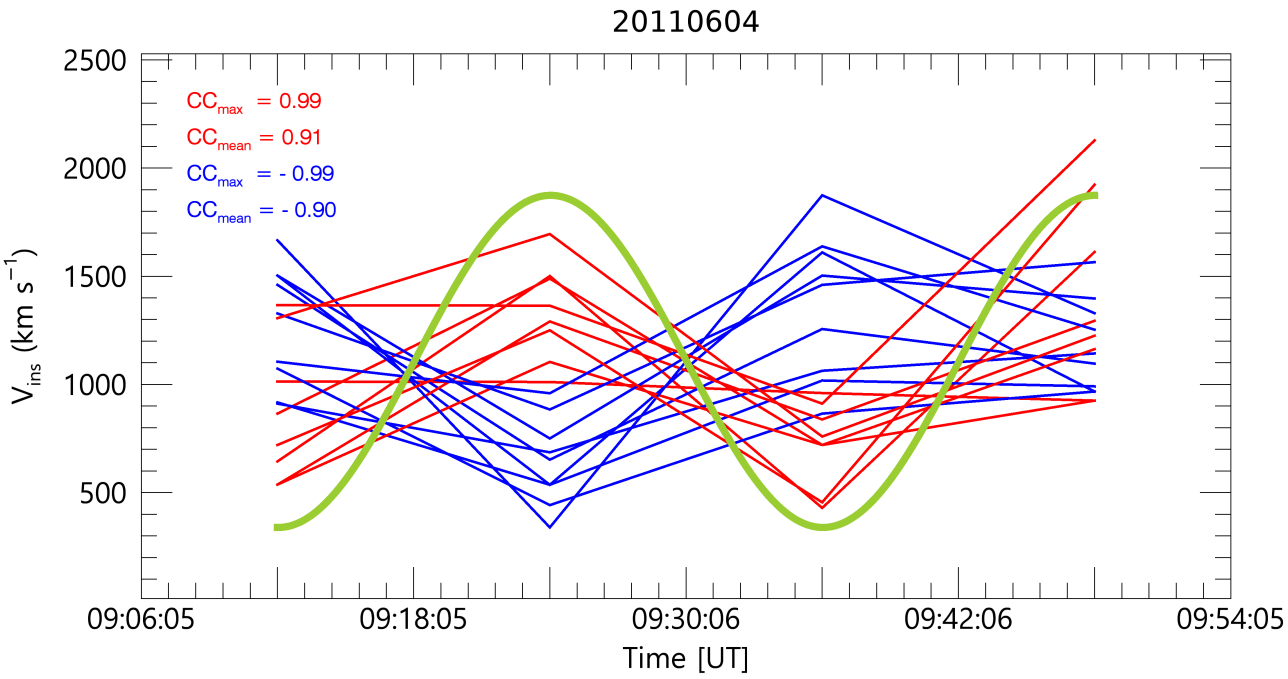

Figure 2. Profiles of the instantaneous projected speeds measured along different azimuthal angles in the 2011 June 4 FHCME. Only the speed profiles with the absolute values of the correlation coefficients with the harmonic function shown in green, larger than 0.6 are shown. The red and blue lines show positive and negative correlations, respectively.

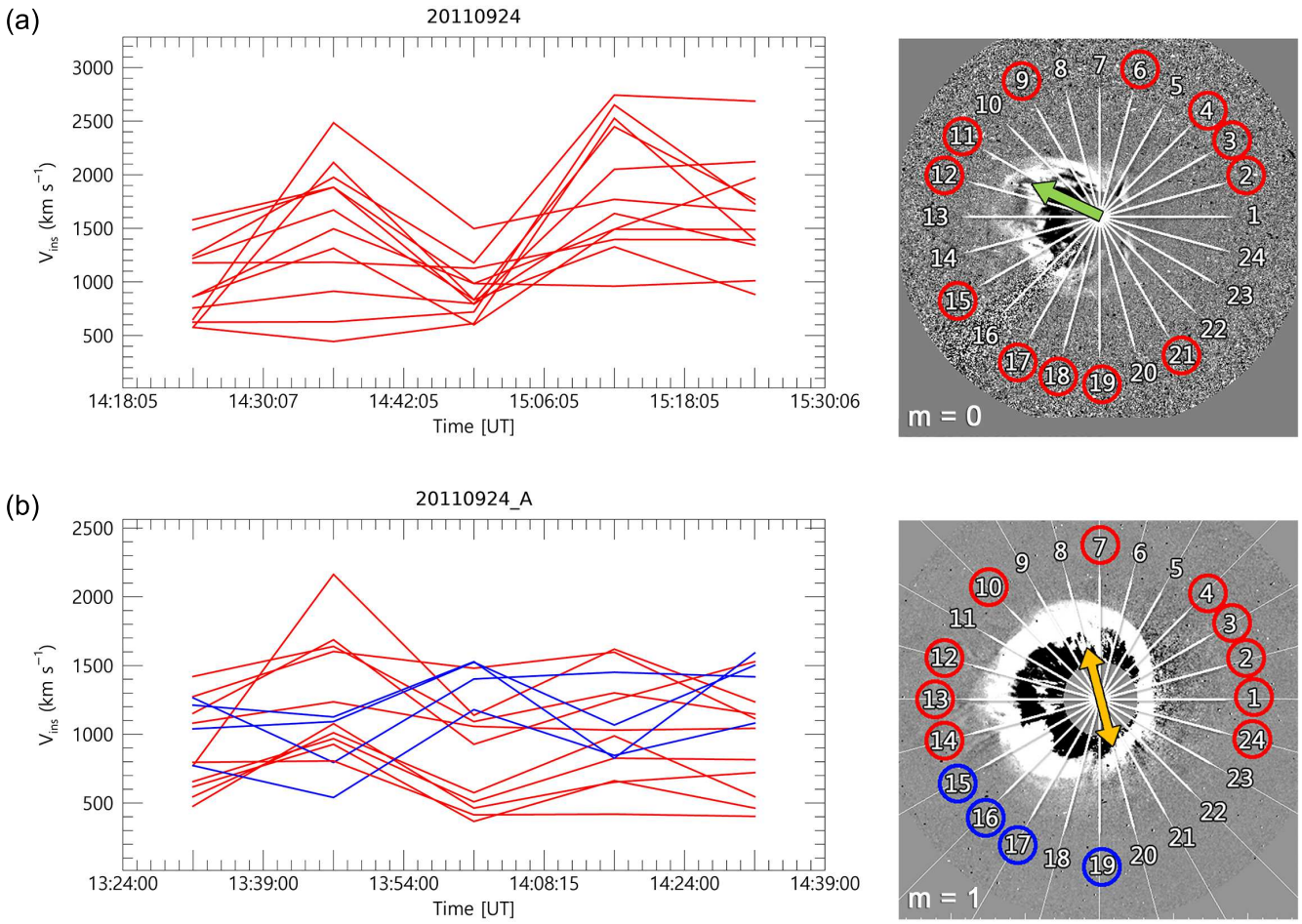

Figure 3. Oscillatory patterns in the 2011 September 24 FHCME (Left), and their azimuthal dependences (Right) observed with: (a) LASCO and (b) STEREO-A. In the left panels, the red and blue lines have the same meaning as in Figure 1. In the right panels, the red and blue circles indicate the azimuths in which the oscillations correlate either positively (red), or negatively (blue) with the best-fitting harmonic function. The yellow and green arrows show the OPAs and MPAs, respectively. In the left bottom, the azimuthal mode numbers are indicated.

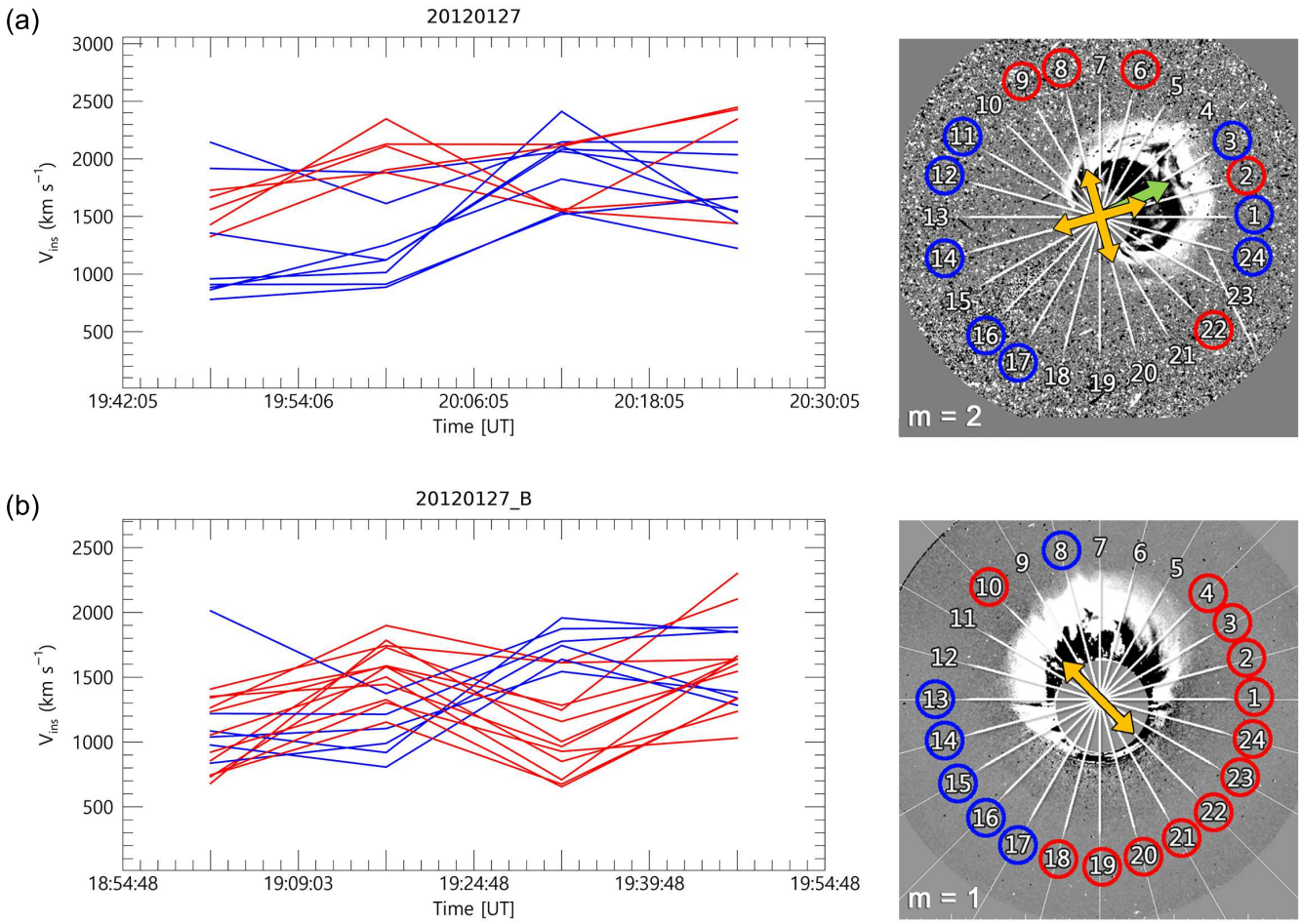

Figure 4. Oscillatory patterns of the 2012 January 27 FHCME (Left) and its azimuthal dependence (Right) observed with: (a) LASCO, and (b) STEREO-B. The notations are the same as in Fig. 3.

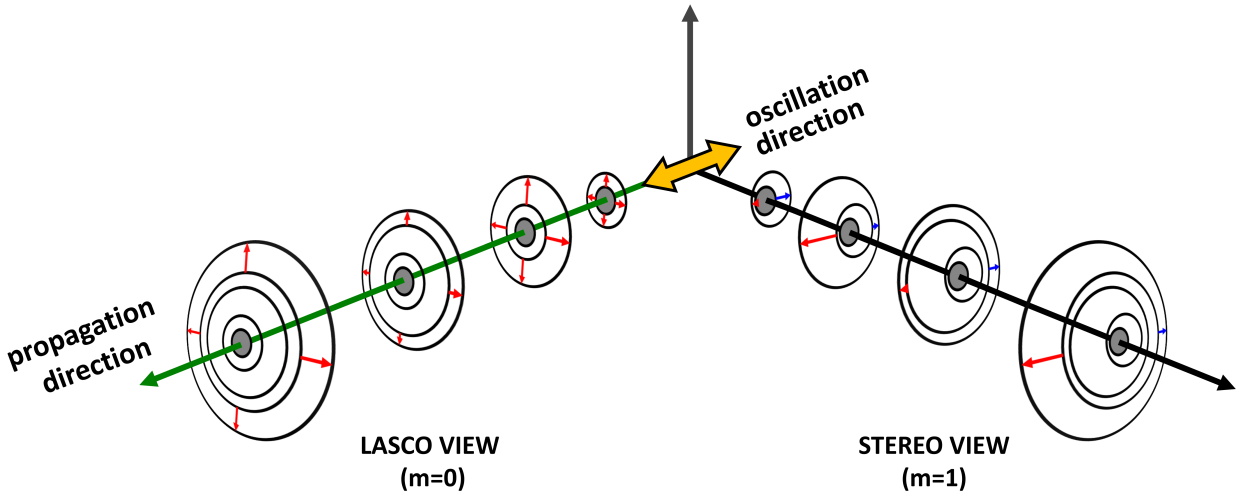

Figure 5. A simplified schematic diagram of the kinematic oscillation of the 2011 September 24 FHCME observed from different angles with two coronagraphs. The yellow arrow indicates the direction of the oscillation. The green arrow corresponds to the propagation direction of the FHCME. The red and blue arrows show the variation of the instantaneous projected speeds which have two opposite phases: positive correlations at one side of the azimuthal angles and negative correlations at the other side.

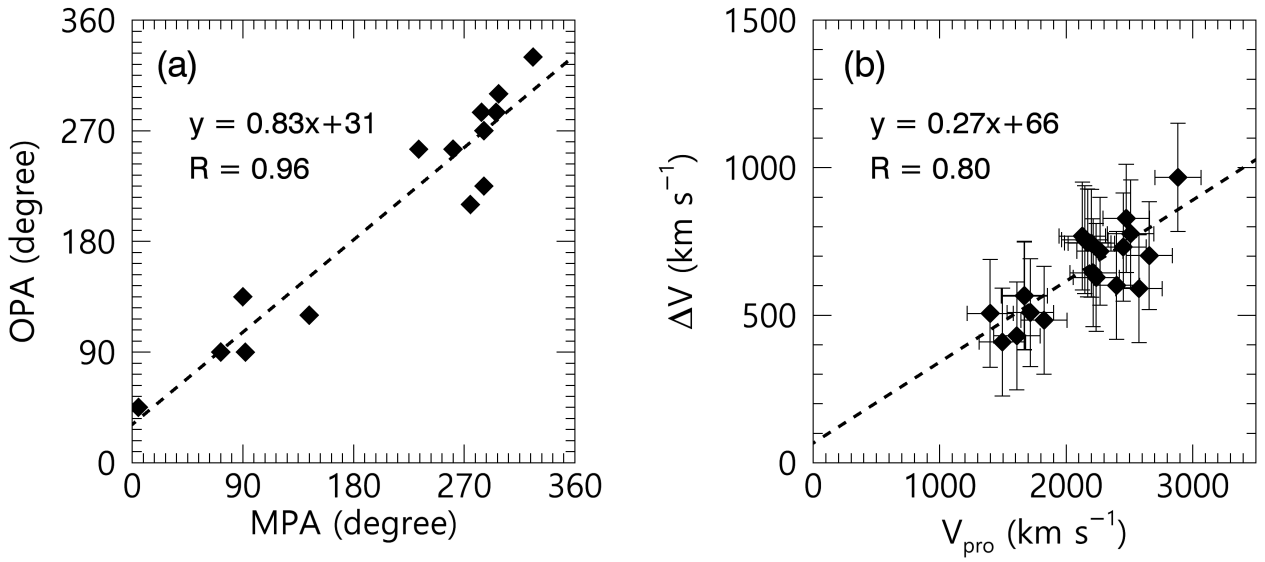

Figure 6. Correlations of various parameters of oscillating FHCMEs from LASCO C3: (a) MPA and OPA and (b) the observed maximum projected speed ($V_{\rm pro}$) and the oscillation amplitude (ΔV). The dashed lines indicate linear fits to the data. The error bars correspond to the standard deviations of the speeds from five independent measurements of the instantaneous height.

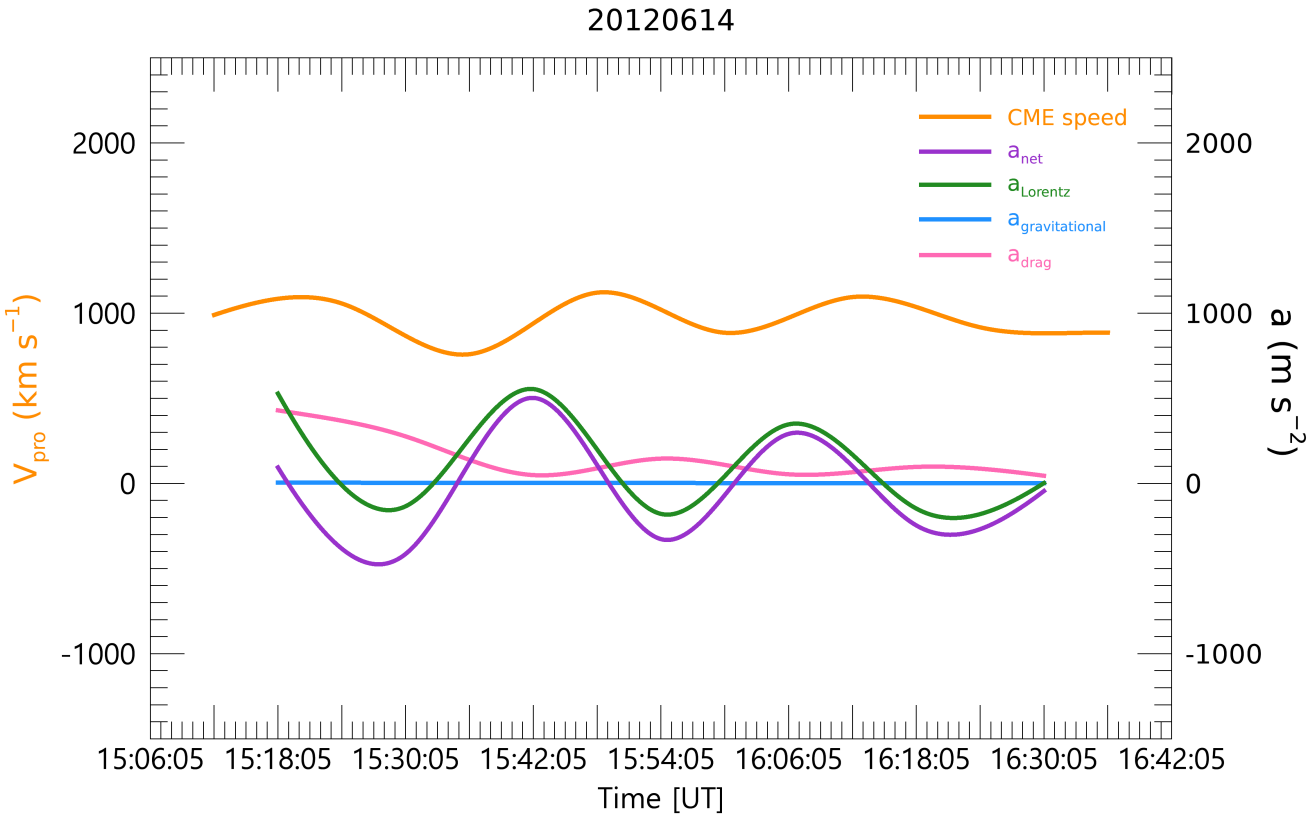

Figure 7. Profiles of the instantaneous projected speed and acceleration of the 2012 March 10 event from LASCO C3. The orange line indicates the maximum projected speed of the CME. The purple, green, blue and pink correspond to the net, Lorentz, gravitational, and solar wind drag acceleration of the CME.